

## Large-scale synthesis of single-crystalline $\beta$ -Ga<sub>2</sub>O<sub>3</sub> nanoribbons, nanosheets and nanowires

This article has been downloaded from IOPscience. Please scroll down to see the full text article.

2001 J. Phys.: Condens. Matter 13 L937

(<http://iopscience.iop.org/0953-8984/13/48/103>)

View [the table of contents for this issue](#), or go to the [journal homepage](#) for more

Download details:

IP Address: 171.66.16.238

The article was downloaded on 17/05/2010 at 04:36

Please note that [terms and conditions apply](#).

## LETTER TO THE EDITOR

## Large-scale synthesis of single-crystalline $\beta$ -Ga<sub>2</sub>O<sub>3</sub> nanoribbons, nanosheets and nanowires

Jianye Li<sup>1,2</sup>, Xiaolong Chen<sup>1</sup>, Zhiyu Qiao<sup>2</sup>, Meng He<sup>1</sup> and Hui Li<sup>1</sup>

<sup>1</sup> Institute of Physics and Centre for Condensed Matter Physics, Chinese Academy of Sciences, PO Box 603-23, Beijing 100080, People's Republic of China

<sup>2</sup> Department of Physical Chemistry, University of Science and Technology Beijing, Beijing 100083, People's Republic of China

E-mail: jianyeli@21cn.com

Received 29 August 2001, in final form 29 October 2001

Published 16 November 2001

Online at [stacks.iop.org/JPhysCM/13/L937](http://stacks.iop.org/JPhysCM/13/L937)

### Abstract

Through a simple gas reaction, single-crystalline  $\beta$ -Ga<sub>2</sub>O<sub>3</sub> nanoribbons, nanosheets and nanowires were synthesized on a large scale at 700 °C. They were characterized by means of x-ray powder diffraction (XRD), field emission scanning electron microscopy (FE-SEM), energy-dispersive x-ray spectroscopy (EDS), transmission electron microscopy (TEM), high-resolution transmission electron microscopy (HRTEM), selected-area electron diffraction (SAED) and Raman spectroscopy. FE-SEM and TEM images showed that the product was composed of nanoribbons, nanosheets and nanowires. XRD, EDS, HRTEM, SAED and the Raman spectrum indicated that all of the nanoribbons, nanosheets and nanowires were of single-crystalline  $\beta$ -Ga<sub>2</sub>O<sub>3</sub>.

Metal oxides play an important role in many scientific and technological fields [1].  $\beta$ -Ga<sub>2</sub>O<sub>3</sub>, having one of the widest band gaps among oxides with semiconducting properties, is a very promising candidate for use as an ultraviolet transparent conducting oxide (TCO) in excimer laser and other applications [2]. In the past few years, much effort has been devoted to the study of  $\beta$ -Ga<sub>2</sub>O<sub>3</sub> low-dimensional-structure materials, and  $\beta$ -Ga<sub>2</sub>O<sub>3</sub> nanowires have been obtained through physical evaporation [3] and arc-discharge [4] methods.

A nanobelt (or nanoribbon) exhibits a different morphology to a nanotube or nanowire, and has a high ratio of area to volume [5, 6]. Nanobelts (or nanoribbons) could represent an ideal system for investigating to achieve a full understanding of dimensionally confined transport phenomena in semiconductors and building functional devices using individual nanobelts (or nanoribbons) [6]. We have fabricated GaN nanoribbons by a sublimation process [7]. Recently, Pan *et al* [6] synthesized nanometre-scale belt-like (or ribbon-like) semiconducting oxides by evaporating the desired metal oxide powders at high temperatures and this has attracted a great deal of attention [5]. Through a simple but effective gas reaction method, we synthesized single-crystalline  $\beta$ -Ga<sub>2</sub>O<sub>3</sub> nanoribbons, nanosheets and nanowires on a large scale at a relatively low temperature. Here we report the results.

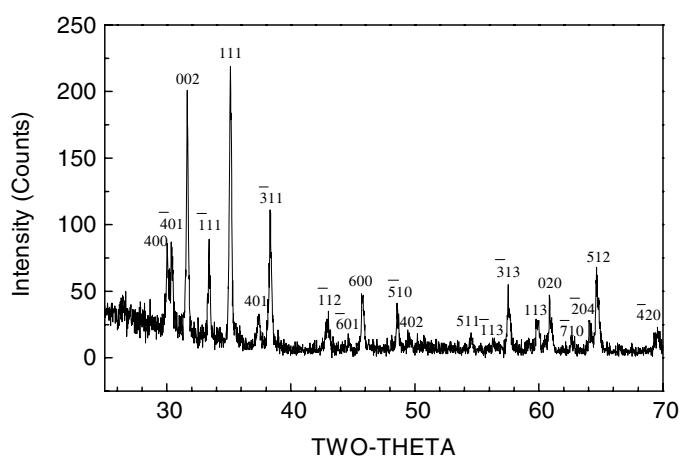
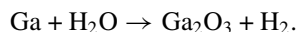


**Figure 1.** A typical powder XRD pattern of the product obtained using Cu  $K\alpha$  radiation.

The system that we use to synthesize  $\beta$ - $\text{Ga}_2\text{O}_3$  nanoribbons, nanosheets and nanowires is basically similar to that designed to form GaN nanowires [8]. The reaction can be expressed as



The reaction was carried out in a conventional tube furnace with a horizontal quartz glass tube. The length of the quartz glass tube is 1.1 m. First, a silicon substrate was quickly dipped in a  $\text{Ni}(\text{NO}_3)_2$  ethanol solution (the concentration was 0.01 M) [8]. After drying in air, the silicon substrate and 4 g of gallium metal with a separation of 10 mm were put in a quartz glass boat and the boat was loaded into the centre of a quartz glass tube. The tube was placed in a conventional tube furnace. 20 ml water in a beaker was placed in the entrance to the quartz glass tube. The quartz tube was first pumped, then filled with inert argon gas, and then re-pumped. This operation was repeated three times. After that, the quartz tube was heated under an argon flow of about  $50 \text{ cm}^3 \text{ min}^{-1}$ . When  $700^\circ\text{C}$  was reached, the temperature was kept constant for 30 min, and then the power was turned off. Upon cooling to room temperature, a white layer on the substrate was formed.

The x-ray powder diffraction (XRD) of the product was characterized using a Rigaku (Tokyo, Japan) D/max-2400 x-ray diffractometer with Cu  $K\alpha$  radiation.

Figure 1 shows a typical powder XRD pattern of the white layer. The (400), ( $\bar{4}01$ ), (002), ( $\bar{1}11$ ), (111), (401), ( $\bar{3}11$ ), ( $\bar{1}12$ ), (601), (600), (510), (402), (511), ( $\bar{1}13$ ), ( $\bar{3}13$ ), (113), (020), ( $\bar{7}10$ ), ( $\bar{2}04$ ), (512), ( $\bar{4}20$ ) XRD reflection peaks correspond to the monoclinic  $\text{Ga}_2\text{O}_3$  (or  $\beta$ - $\text{Ga}_2\text{O}_3$ ) phase. The positions of the XRD peaks show good agreement with those for monoclinic structure  $\text{Ga}_2\text{O}_3$  with the lattice constants  $a = 12.23 \text{ \AA}$ ,  $b = 3.04 \text{ \AA}$ ,  $c = 5.80 \text{ \AA}$ ,  $\alpha = 90^\circ$ ,  $\beta = 103.7^\circ$  and  $\gamma = 90^\circ$  [9]. The XRD result reveals that  $\beta$ - $\text{Ga}_2\text{O}_3$  has been obtained.

The morphologies of the product were observed using a Hitachi (Tokyo, Japan) S-4200 field emission scanning electron microscope (FE-SEM) equipped with an energy-dispersive x-ray spectroscopy (EDS).

Figures 2–4 show FE-SEM images of different areas of a layer deposited on a substrate:  $\beta$ - $\text{Ga}_2\text{O}_3$  nanoribbons, nanosheets and nanowires are present. At different sites, different morphological types ( $\beta$ - $\text{Ga}_2\text{O}_3$  nanoribbons, nanosheets and nanowires) dominate and there is no regularity. As seen in the FE-SEM image shown in figure 2, the main morphological type is  $\beta$ - $\text{Ga}_2\text{O}_3$  nanoribbons and the widths and the thicknesses of the nanoribbons are 50 nm– $1 \mu\text{m}$  and 5–50 nm respectively. Most of them are very long, and the maximum length is  $800 \mu\text{m}$ . The

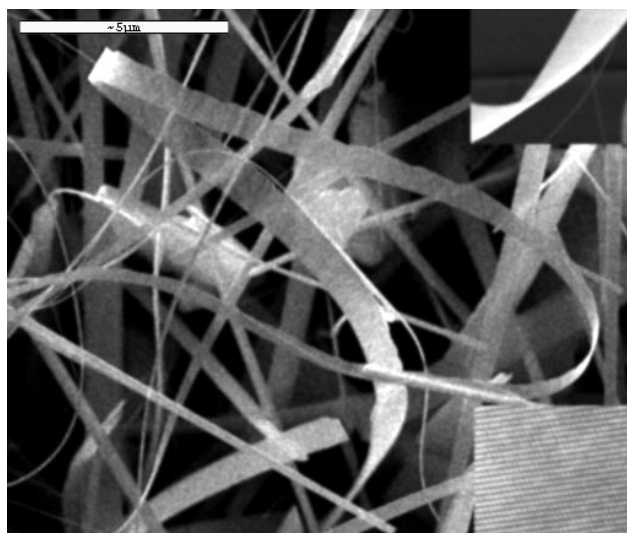


**Figure 2.** An FE-SEM image of  $\beta$ -Ga<sub>2</sub>O<sub>3</sub> nanoribbons. The upper and lower insets show a high-magnification FE-SEM image and an HRTEM lattice image of a  $\beta$ -Ga<sub>2</sub>O<sub>3</sub> nanoribbon respectively.

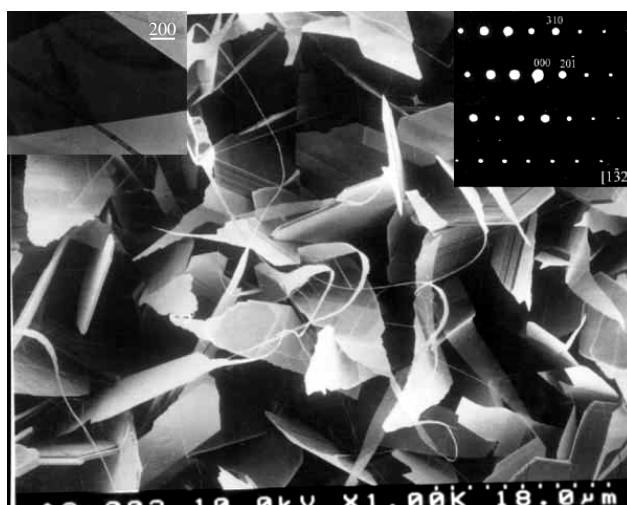


**Figure 3.** An FE-SEM image of  $\beta$ -Ga<sub>2</sub>O<sub>3</sub> sheets. The left and right insets show a TEM image and a [1132] SAED pattern of a  $\beta$ -Ga<sub>2</sub>O<sub>3</sub> nanosheet respectively.

upper inset of figure 2 shows a high-magnification FE-SEM image of a  $\beta$ -Ga<sub>2</sub>O<sub>3</sub> nanoribbon with width and thickness of about 600 and 40 nm respectively. Figure 3 shows a morphological image of  $\beta$ -Ga<sub>2</sub>O<sub>3</sub> sheets with thickness on the nanometre scale. The thicknesses of most of the nanosheets lie in the range 10–100 nm, and the maximum length exceeds 100  $\mu$ m. The thickness, length and width of the nanosheets increase with the reaction time. In figure 4,  $\beta$ -Ga<sub>2</sub>O<sub>3</sub> nanowires dominate. The diameters of the nanowires are about 5–90 nm and the maximum length is more than 600  $\mu$ m.

EDS measurements indicate that all of the nanoribbons, nanosheets and nanowires consist of Ga and O with an atomic ratio of 2:3, corresponding to the chemical composition of Ga<sub>2</sub>O<sub>3</sub>.

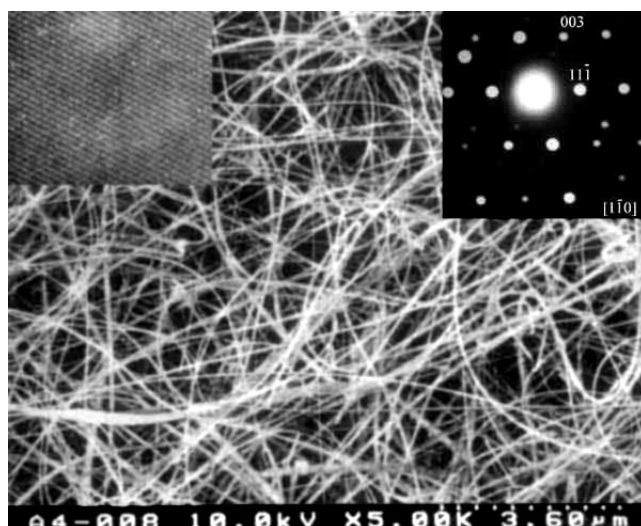


**Figure 4.** An FE-SEM image of  $\beta$ -Ga<sub>2</sub>O<sub>3</sub> nanowires. The left and right insets show an HRTEM lattice image and a  $[1\bar{1}0]$  SAED pattern of a  $\beta$ -Ga<sub>2</sub>O<sub>3</sub> nanowire respectively.

The high-resolution transmission electron microscopy (HRTEM) images, the transmission electron microscopy (TEM) image and the typical selected-area electron diffraction (SAED) patterns of the product were taken with a Jeol-2010 TEM.

The lower inset of figure 2 shows an HRTEM lattice image of a  $\beta$ -Ga<sub>2</sub>O<sub>3</sub> nanoribbon, and it shows that the  $\beta$ -Ga<sub>2</sub>O<sub>3</sub> nanoribbons are uniform in structure and single crystalline. The HRTEM image also indicates that the nanoribbon is solid, not hollow. The left inset of figure 3 shows a TEM image of a  $\beta$ -Ga<sub>2</sub>O<sub>3</sub> nanosheet, and it shows that the nanosheet is solid nature inside. The right inset of figure 3 shows a  $[1\bar{3}2]$  SAED pattern of a  $\beta$ -Ga<sub>2</sub>O<sub>3</sub> nanosheet. The pattern is consistent with Ga<sub>2</sub>O<sub>3</sub> single crystal, indexed according to a monoclinic cell with lattice parameters of  $a = 12.23 \text{ \AA}$ ,  $b = 3.04 \text{ \AA}$ ,  $c = 5.80 \text{ \AA}$ ,  $\alpha = 90^\circ$ ,  $\beta = 103.7^\circ$  and  $\gamma = 90^\circ$ , consistent with the above XRD results. The insets of figure 4 show the HRTEM image (left) and  $[1\bar{1}0]$  SAED pattern (right) of a  $\beta$ -Ga<sub>2</sub>O<sub>3</sub> nanowire, and they confirm that the nanowires are uniform in structure and composed of single-crystal monoclinic  $\beta$ -Ga<sub>2</sub>O<sub>3</sub>. The HRTEM image and SAED pattern of the nanowire also verify the above XRD results.

The Raman spectrum was recorded at room temperature with a Spex-1403 Raman spectrometer using the 488 nm line of an Ar<sup>+</sup> laser as the excitation source. Figure 5 shows the Raman spectrum of the white product scraped from the silicon substrate. Several sharp peaks at 144, 169, 200, 320, 346, 416, 475, 629, 655 and 766 cm<sup>-1</sup> are observed. The peak positions for the product are in good agreement with those reported in the literature [3,4]. The Raman measurement also proves that the product deposited on the substrate is  $\beta$ -Ga<sub>2</sub>O<sub>3</sub>.

Through a simple gas reaction and at a relatively low temperature, different morphologies of single-crystalline  $\beta$ -Ga<sub>2</sub>O<sub>3</sub> low-dimensional materials including nanoribbons, nanosheets and nanowires were synthesized on a large scale on the same silicon substrate. Using a similar method, we also fabricated  $\beta$ -Ga<sub>2</sub>O<sub>3</sub> nanosheets on a specially treated quartz glass substrate and found that nanosheets were the major products. The present approach may be expanded to form nanoribbons, nanowires and, in particular, sheets of other materials for use in fundamental research and technological applications. We found that the size of the  $\beta$ -Ga<sub>2</sub>O<sub>3</sub> nanosheets increase with the reaction time. Perhaps with some improvement, the  $\beta$ -Ga<sub>2</sub>O<sub>3</sub> nanosheets

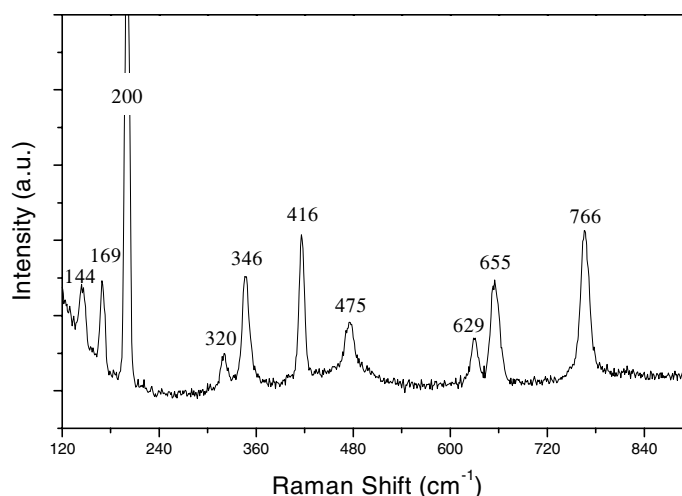


**Figure 5.** A Raman scattering spectrum of  $\beta$ -Ga<sub>2</sub>O<sub>3</sub> low-dimensional materials including nanoribbons, nanosheets and nanowires.

can be developed into  $\beta$ -Ga<sub>2</sub>O<sub>3</sub> films; this suggests a wide range of potential fabrications of films of  $\beta$ -Ga<sub>2</sub>O<sub>3</sub> and other materials for applications.

This project was financially supported by the National Natural Science Foundation of China (NSFC) and the Chinese Academy of Sciences (CAS). Ms C Y Wang and Mr T S Ning are acknowledged for their help in the work.

## References

- [1] Schmitz G, Gassmann P and Franchy R 1998 *J. Appl. Phys.* **83** 2533
- [2] Ueda N, Hosono H, Waseda R and Kawazoe H 1997 *Appl. Phys. Lett.* **71** 933
- [3] Zhang H Z, Kong Y C, Wang Y Z, Du X, Bai Z G, Wang J J, Yu D P, Ding Y, Hang Q L and Feng S Q 1999 *Solid State Commun.* **109** 677
- [4] Choi Y C, Kim W S, Park Y S, Lee S M, Bae D J, Lee Y H, Park G, Choi W B, Lee N S and Kun J M 2000 *Adv. Mater.* **12** 746
- [5] Szuromi P 2001 *Science* **291** 1855
- [6] Pan Z W, Dai Z R and Wang Z L 2001 *Science* **291** 1947
- [7] Li J Y, Qiao Z Y, Chen X L, Cao Y G, Lan Y C and Wang C Y 2000 *Appl. Phys. A* **71** 587
- [8] Chen X L, Li J Y, Cao Y G, Lan Y C, Li H, He M, Wang C Y, Zhang Z and Qiao Z Y 2000 *Adv. Mater.* **12** 1432
- [9] JCPDS 2000 *Powder Diffraction Data Cards* JCPDS International Centre for Diffraction Data, Swarthmore, PA